

## Nanoscale magnetic tunnel junction sensors with perpendicular anisotropy sensing layer

Z. M. Zeng,<sup>1,2</sup> P. Khalili Amiri,<sup>3</sup> J. A. Katine,<sup>4</sup> J. Langer,<sup>5</sup> K. L. Wang,<sup>3</sup> and H. W. Jiang<sup>1</sup>

<sup>1</sup>Department of Physics and Astronomy, University of California, Los Angeles, California 90095, USA

<sup>2</sup>Suzhou Institute of Nano-Tech and Nano-Bionics, Chinese Academy of Sciences, Ruoshui Road 398, 215123 Suzhou, People's Republic of China

<sup>3</sup>Department of Electrical Engineering, University of California, Los Angeles, California 90095, USA

<sup>4</sup>Hitachi Global Storage Technologies, San Jose, California 95135, USA

<sup>5</sup>Singulus Technologies, 63796 Kahl am Main, Germany

(Received 14 May 2012; accepted 25 July 2012; published online 7 August 2012)

A nano-scale linear magnetoresistance sensor is demonstrated using magnetic tunnel junctions with an in-plane magnetized reference layer and a sensing layer with interfacial perpendicular anisotropy. We show that the sensor response depends critically on the thickness of the sensing layer since its perpendicular anisotropy is significantly associated with thickness. The optimized sensors exhibit a large field sensitivity of up to 0.02% MR/Oe and a high linear field range of up to 600 Oe. These findings imply that this sensing scheme is a promising method for developing nano-scale magnetic sensors with simple design, high sensitivity, and low power consumption. © 2012 American Institute of Physics. [<http://dx.doi.org/10.1063/1.4744914>]

Magneto-resistance (MR) sensors based on spin valve and magnetic tunnel junction (MTJ) devices have been widely used in applications such as field sensors, position and rotation sensors, as well as medical applications because of their large signal, low power consumption, and long endurance.<sup>1</sup> In magnetic sensors, the central issue is the linear and reversible response to the magnetic medium. At present, one popular method is to align the magnetizations of a sensing layer and a reference layer to be initially perpendicular to each other in the plane of the film. This can be obtained by introducing an external or internal transverse bias field,<sup>2,3</sup> or by utilizing the shape anisotropy<sup>4</sup> and step edge anisotropy.<sup>5</sup> However, such designs complicate sensor design, and suffer from magnetization fluctuation and magnetic noise when reducing sensor size. This limits the scalability and integration for future applications. An alternative method is to harness superparamagnetic-like behavior<sup>6–9</sup> as the thickness of the sensing layer is reduced to a certain critical value, e.g., 1.0 nm<sup>6</sup> or 1.5 nm.<sup>7</sup> In addition, there is another approach that employs out-of-plane magnetized materials to achieve a linear and hysteresis-free response.<sup>10–14</sup> For example, the linear response and large linear field range have been obtained in sensors with a perpendicularly magnetized reference layer and in-plane sensing layer.<sup>10,12</sup> A sensor with a high linearity up to applied field of 500 Oe was demonstrated by using Pt/CoFe out-of-plane magnetized sensing layer.<sup>13,14</sup> However, the Pt-multilayer structures always exhibit small MR due to their low spin polarization, further resulting in low sensitivity.

Recently, Fe-rich CoFeB materials have been used for MgO based MTJs in various applications such as memories<sup>15–17</sup> and microwave oscillators,<sup>18,19</sup> exhibiting high MR value and large interfacial perpendicular anisotropy (IPA). The utilization of CoFeB with large IPA for building sensors is expected to produce high sensitivity due to its high MR ratio when used in MgO based MTJ structures. In this study, we report nanoscale MTJ sensors with a CoFeB sensing layer

that exhibits perpendicular anisotropy. The sensor structure and magnetic configuration are illustrated in Fig. 1(a). The reference layer consists of a synthetic antiferromagnetic layer and the magnetization of the Co-rich Co<sub>60</sub>Fe<sub>20</sub>B<sub>20</sub> reference layer is aligned parallel to the film plane. The wedge Co<sub>20</sub>Fe<sub>60</sub>B<sub>20</sub> ( $t_{CoFeB} = 1.30\text{--}1.85$  nm) sensing layer is designed to tune its perpendicular anisotropy by changing the thickness of the sensing layer.<sup>16,17</sup> Below a certain transition thickness, the magnetization of the sensing layer is perpendicular to the film plane. In this scheme, there is no need for a sensor with a large aspect ratio or external bias field, which is necessary for in-plane sensors in order to achieve linear output. The design provides better scalability, simple structure, and high sensitivity. Furthermore, the tunability of the perpendicular anisotropy of the CoFeB layer by adjusting its thickness allows one to easily design various magnetic sensors for specific applications.

The magnetic multilayers were deposited on a Si/SiO<sub>2</sub> substrate in a Singulus TIMARIS physical vapor deposition (PVD) system. The completed stack was annealed for 2 h at 300 °C in 1 T. Electron-beam lithography and ion milling were used to define and etch the MTJ layers resulting in circular nanopillars with nominal diameters of 60 nm, 80 nm, and 100 nm. The experimental results for the devices with the different diameters show similar behavior and all data shown below are for 80 nm circular nanopillars. The magneto-transport measurements were performed by a G-S-G probe at room temperature.

Figures 1(b)–1(f) show the resistance as a function of applied magnetic field for different sensing layer thickness ( $t_{CoFeB}$ ). For the device with  $t_{CoFeB} = 1.84$  nm, normal MR behavior was observed with MR ratio of 82% [ $MR = (R_{AP} - R_P)/R_P$ , where  $R_{AP}$  and  $R_P$  are the resistances for an anti-parallel and parallel magnetization configuration, respectively], which suggests that the magnetization of the CoFeB sensing layer is in the plane of the films. The slight shift in the MR curve is presumably due to the interlayer coupling,

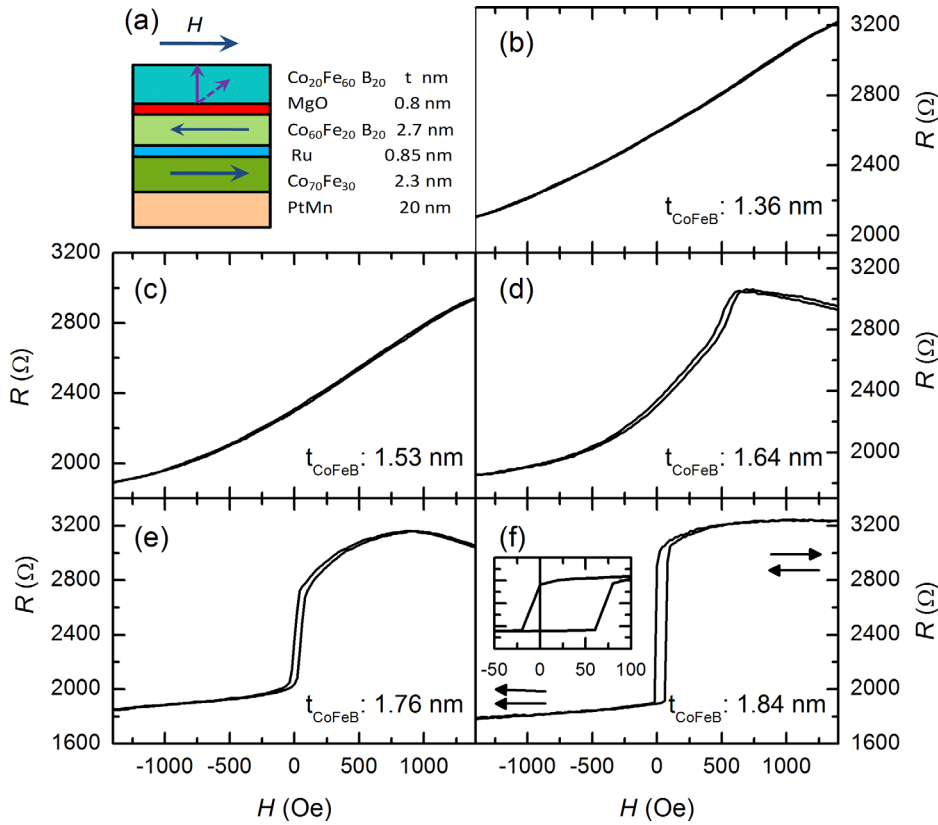


FIG. 1. (a) Layer structure and magnetic configuration of sensors. (b)-(f) Resistance as a function of the applied magnetic field for the sensors with different thickness ( $t_{\text{CoFeB}}$ ) of the sensing CoFeB layer. The inset in (f) shows the minor loop.

such as orange peel coupling, between the reference and the sensing layers (this can be eliminated by choosing a compensated synthetic antiferromagnet for the pinned layer).<sup>6</sup> With decreasing  $t_{\text{CoFeB}}$ , the out-of-plane magnetization component of the sensing layer continues to increase, and for  $t_{\text{CoFeB}} = 1.64$  nm, the linear response around zero field with hysteretic behavior is presented as shown in Fig. 1(d), indicating that the CoFeB sensing layer exhibits a transition from in-plane magnetization to out-of-plane magnetization in zero-applied magnetic field. Further decreasing of the thickness of the CoFeB sensing layer to  $t_{\text{CoFeB}} = 1.53$  nm, the sensor response is linear and hysteresis-free around zero-applied field, indicating a stable single domain state. At  $t_{\text{CoFeB}} = 1.36$  nm, the linearity extends to a large applied field of more than 1000 Oe. This CoFeB thickness dependence of the MR loops is consistent with that in Ref. 14, correlating to the perpendicular anisotropy at CoFeB/MgO interface that has been confirmed by VSM measurement.<sup>17</sup>

Figure 2(a) shows the MR ratio as a function of the applied magnetic field for a sensor with  $t_{\text{CoFeB}} = 1.36$  nm at a field of  $-400 \text{ Oe} \leq H \leq 400 \text{ Oe}$ , which indicates that the magnetic field sensitivity is 0.017% MR/Oe. This value is significantly larger than that (0.0018% MR/Oe) previously reported for a sensor utilizing an out-of-plane magnetized sensing layer<sup>14</sup> because of the significantly enhanced MR ratio in our case. The nonlinearity, defined as  $100 \times [R(H) - R_0 - r_0 H] / R(H)$ ,<sup>12</sup> is plotted in Fig. 2(b), where  $R_0$  and  $r_0$  are coefficients obtained from linear regression of  $R(H)$  as a function of the applied magnetic field  $H$ . The nonlinearity depends strongly on the CoFeB sensing layer thickness. To better understand the  $t_{\text{CoFeB}}$  dependence of the field sensitivity and field sensing range, the data corresponding to the nonlinearity of smaller than 1% were chosen for quantitative

analysis. The linear field range increases while the field sensitivity decreases with decreasing  $t_{\text{CoFeB}}$  as shown in Fig. 3. For  $t_{\text{CoFeB}} = 1.64$  nm, the field sensitivity is up to 0.036% MR/Oe, but the linear field range is limited to 150 Oe. This is, however, larger than the range reported for sensors (0.0047% MR/Oe) with super-paramagnetic CoFeB layer with a similar field range.<sup>6</sup> When the CoFeB sensing layer thickness is less than 1.53 nm, the field sensitivity only shows a small reduction (from 0.019% MR/Oe at 1.53 nm to 0.0165% MR/Oe at 1.36 nm). The linear field range substantially increases from 450 to 650 Oe as the CoFeB sensing layer decreases from 1.53 to 1.36 nm. This changed trend is similar to that reported by van Dijken and Coey<sup>14</sup> for their spin valve sensors with out-of-plane Pt/CoFe sensing layer, but a higher field sensitivity can be obtained in our sensors due to the larger MR effect with MgO barrier and high spin polarization CoFeB layer. Note that the linear field range is considerably larger than that for sensors utilizing an external field (less than 10 Oe),<sup>2</sup> shape anisotropy,<sup>4</sup> and super-paramagnetic layers.<sup>6</sup>

We will next discuss the underlying mechanisms of the  $t_{\text{CoFeB}}$  dependence of the field sensitivity and nonlinearity. In our case, where the magnetization of the sensing free layer is expected to coherently rotate toward the film plane, the resulting change in the sensor resistance is expressed as<sup>14</sup>

$$\frac{R(H) - R(0)}{R(0)} = \frac{R_P - R_{AP}}{R_{AP} + R_P} \sin\left(\tan^{-1}\left(\frac{H}{H_K}\right)\right) = \frac{1}{1 + \frac{2}{MR}} \sin\left(\tan^{-1}\left(\frac{H}{H_K}\right)\right), \quad (1)$$

where  $H_K = 2K/\mu_0 M_s$ ,  $K = K_i/t_{\text{CoFeB}} - M_s^2/\mu_0$ ,  $\mu_0$  is permeability in free space,  $M_s$  is the saturation magnetization, and

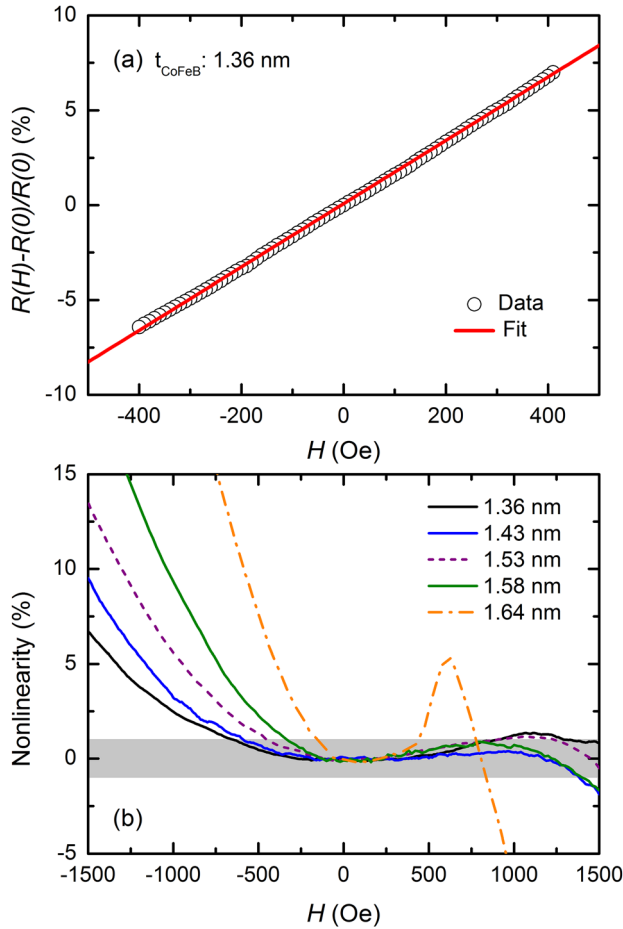


FIG. 2. (a) Resistance as a function of applied magnetic field curve for a sensor with CoFeB sensing layer of  $t_{\text{CoFeB}} = 1.36$  nm in the low magnetic field regime. (b) Nonlinearity in the magnetoresistance for different CoFeB sensing layer thickness. The light gray box in (b) illustrates the range where nonlinearity is less than 1%.

$K_i$  is the interfacial perpendicular anisotropy. Thus for small rotation angles, the field sensitivity can be written as

$$S = \frac{1}{R(0)} \frac{dR}{dH} = \frac{R_{AP} - R_P}{R_{AP} + R_P} \frac{1}{H_k} = \frac{1}{1 + \frac{2}{MR} H_k}. \quad (2)$$

From Eq. (2), the field sensitivity is dependent on the MR ratio and  $H_k$ . However, in our case, the MR ratio does not change significantly, while  $H_k$  increases strongly as the CoFeB sensing layer thickness is reduced.<sup>17</sup> Therefore,  $H_k$  is dominant in the  $t_{\text{CoFeB}}$  dependence of the field sensitivity as shown in the Fig. 3(b). As for nonlinearity, it can be seen from Eq. (1) that the nonlinearity increases as the external magnetic field and MR increase, while it decreases as  $H_k$  increases, i.e., the nonlinearity decreases with the decrease of  $t_{\text{CoFeB}}$  as shown in Fig. 2(b). Optimizing the field sensitivity, field sensing range, linearity, and reversibility (i.e., critical parameters for magnetic field sensors), our results show that, the devices with  $t_{\text{CoFeB}} \leq 1.60$  nm are promising for magnetic field sensors in our case. In addition, the ability of tuning the sensor performance by changing the sensing layer thickness presents a powerful method to design magnetic sensors for specific applications.

In summary, we fabricated nano-scale MTJ sensors with an in-plane magnetized reference layer and a perpendicular

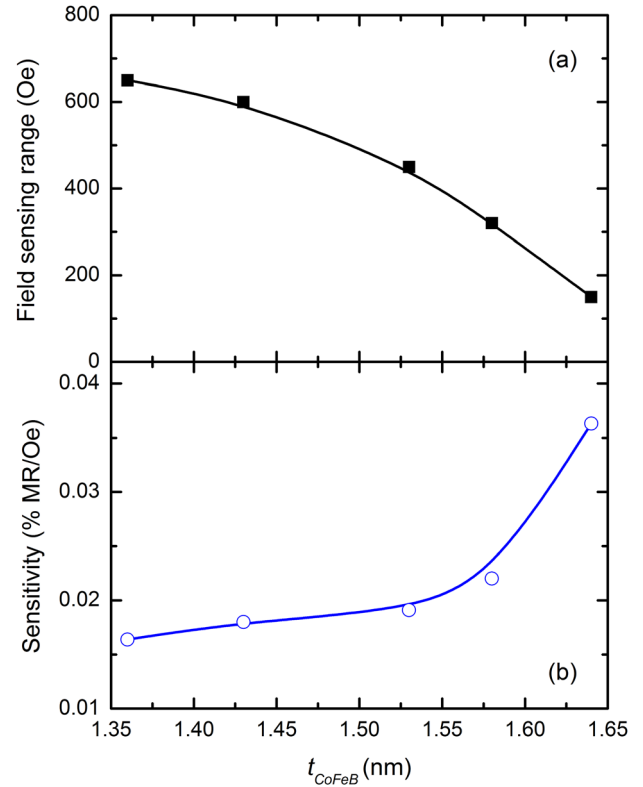


FIG. 3. Field sensing range (a) and sensitivity (b) as a function of the CoFeB sensing layer thickness. The data are deduced from Fig. 2(b) when the nonlinearity is less than 1%. Note that the values corresponding to nonlinearity of 1% for negative fields are smaller than those for positive fields; thus, the negative data are used in this letter. The line in (a) and (b) is a guide for the eye.

anisotropy sensing layer and systematically investigated the effect of thickness of the sensing layer on the magnetic sensor performance. We obtained a sensitivity value of around 0.02% MR/Oe in the nano-scale MTJ with a sensing layer thickness smaller than 1.60 nm. This value is about one order of magnitude larger than the value in previously reported sensors with out-of-plane magnetized sensing layer. Furthermore, we can control the field sensing range only by changing the thickness of the CoFeB sensing layer, which allows the MTJs to be designed for various magnetic field sensors. In addition, the nano-scale size and simple structure of the sensors make them easy to integrate with complementary metal-oxide-semiconductor technology for nano-scale low-power-consumption sensors.

This work was supported by the DARPA STT-RAM and Non-Volatile Logic programs, the Nanoelectronics Research Initiative (NRI) through the Western Institute of Nanoelectronics (WIN), and 100 Talents Programme of the Chinese Academy of Sciences.

<sup>1</sup>J. M. Daughton, A. V. Pohm, R. T. Fayfield, and C. H. Smith, *J. Phys. D* **22**, R169 (1999).

<sup>2</sup>M. Tondra, J. M. Daughton, D. Wang, R. S. Beech, A. Fink, and J. A. Taylor, *J. Appl. Phys.* **83**, 6688 (1998).

<sup>3</sup>X. Y. Liu, C. Ren, and G. Xiao, *J. Appl. Phys.* **92**, 4722 (2002).

<sup>4</sup>Y. Lu, R. A. Altman, S. A. Rishton, P. L. Trouilloud, G. Xiao, W. J. Gallagher, and S. S. P. Parkin, *Appl. Phys. Lett.* **70**, 2610 (1997).

<sup>5</sup>D. Lacour, H. Jaffrès, F. Nguyen Van Dau, F. Petroff, A. Vaurès, and J. Humbert, *J. Appl. Phys.* **91**, 4655 (2002).

- <sup>6</sup>Y. Jang, C. Nam, J. Y. Kim, B. K. Cho, Y. J. Cho, and T. W. Kim, *Appl. Phys. Lett.* **89**, 163119 (2006).
- <sup>7</sup>P. Wisniowski, J. M. Almeida, S. Cardoso, N. P. Barradas, and P. P. Freitas, *J. Appl. Phys.* **103**, 07A910 (2008).
- <sup>8</sup>J. M. Almeida, P. Wisniowski, and P. P. Freitas, *J. Appl. Phys.* **103**, 07E922 (2008).
- <sup>9</sup>W. Shen, B. D. Schrag, A. Girdhar, M. J. Carter, H. Sang, and G. Xiao, *Phys. Rev. B* **79**, 014418 (2009).
- <sup>10</sup>F. B. Mancoff, J. Hunter Dunn, B. M. Clemens, and R. L. White, *Appl. Phys. Lett.* **77**, 1879 (2000).
- <sup>11</sup>W. Jin and Y. W. Liu, *Chin. Phys.* **16**, 1 (2007).
- <sup>12</sup>H. X. Wei, Q. H. Qin, Z. C. Wen, X. F. Han, and X.-G. Zhang, *Appl. Phys. Lett.* **94**, 172902 (2009).
- <sup>13</sup>Y. Ding, J. H. Judy, and J. Wang, *J. Appl. Phys.* **97**, 10N704 (2005).
- <sup>14</sup>S. van Dijken and J. M. D. Coey, *Appl. Phys. Lett.* **87**, 022504 (2005).
- <sup>15</sup>S. Yakata, H. Kubota, Y. Suzuki, K. Yakushiji, A. Fukushima, S. Yuasa, and K. Ando, *J. Appl. Phys.* **105**, 07D131 (2009).
- <sup>16</sup>S. Ikeda, K. Miura, H. Yamamoto, K. Mizunuma, H. D. Gan, M. Endo, S. Kanai, J. Hayakawa, F. Matsukura, and H. Ohno, *Nature Mater.* **9**, 721 (2010).
- <sup>17</sup>P. Khalili Amiri, Z. M. Zeng, J. Langer, H. Zhao, G. Rowlands, Y.-J. Chen, I. N. Krivorotov, J.-P. Wang, H. W. Jiang, J. A. Katine, Y. Huai, K. Galatsis, and K. L. Wang, *Appl. Phys. Lett.* **98**, 112507 (2011).
- <sup>18</sup>Y. Masugata, S. Ishibashi, H. Tomita, T. Seki, T. Nozaki, Y. Suzuki, H. Kubota, A. Fukushima, and S. Yuasa, *J. Phys.: Conf. Ser.* **266**, 012098 (2011).
- <sup>19</sup>Z. M. Zeng, P. Khalili Amiri, I. N. Krivorotov, H. Zhao, G. Finocchio, J.-P. Wang, J. A. Katine, Y. Huai, J. Langer, K. Galatsis, K. L. Wang, and H. W. Jiang, *ACS Nano* **6**, 6115 (2012).